Supporting information for

Changing the chemical and physical properties of high valent heterobimetallic bis-(μ-oxido) Cu-Ni complexes by ligand effects

Maria-Chrysanthi Kafentzi, Maylis Orio, Marius Réglier, Shegnlai Yao, Uwe Kuhlmann, Peter Hildebrandt, Matthias Driess, A. Jalila Simaan and Kallol Ray

I. Additional spectroscopic data for 3b

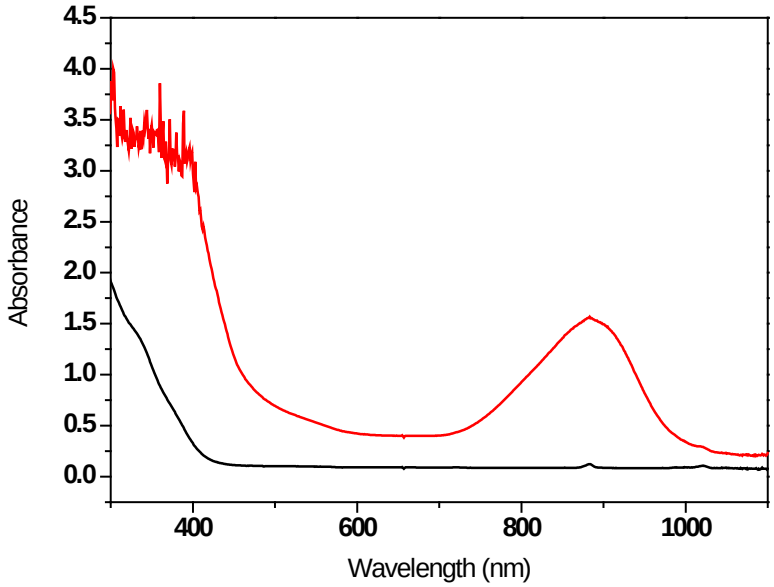

Figure S 1. Absorption spectra of **3a** at -90°C (red) and at -30°C (black) in dichloromethane (0.15 mM).

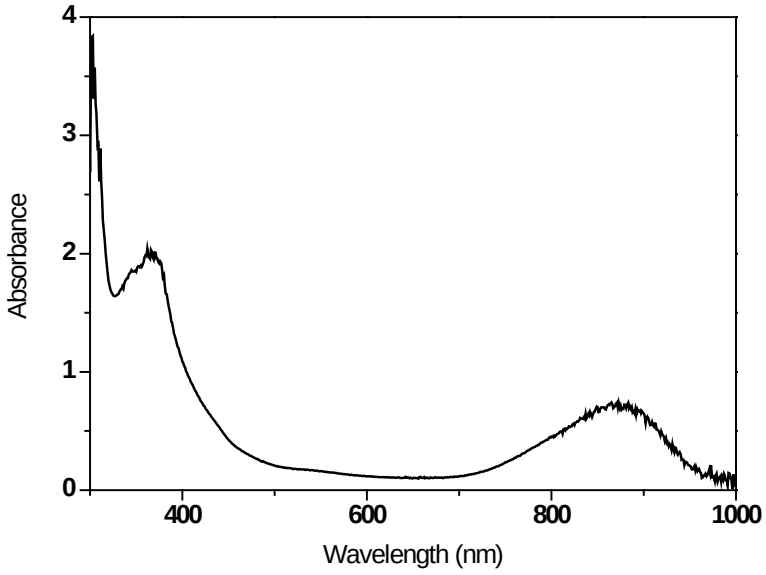

Figure S 2. Absorption spectrum of **3b** at -90°C in dichloromethane (0.1 mM).

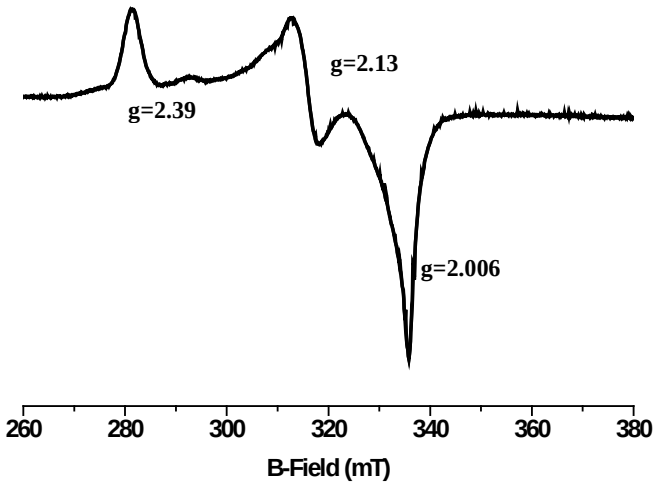

Figure S 3. X-band EPR spectrum of **3b** in dichloromethane at 77K

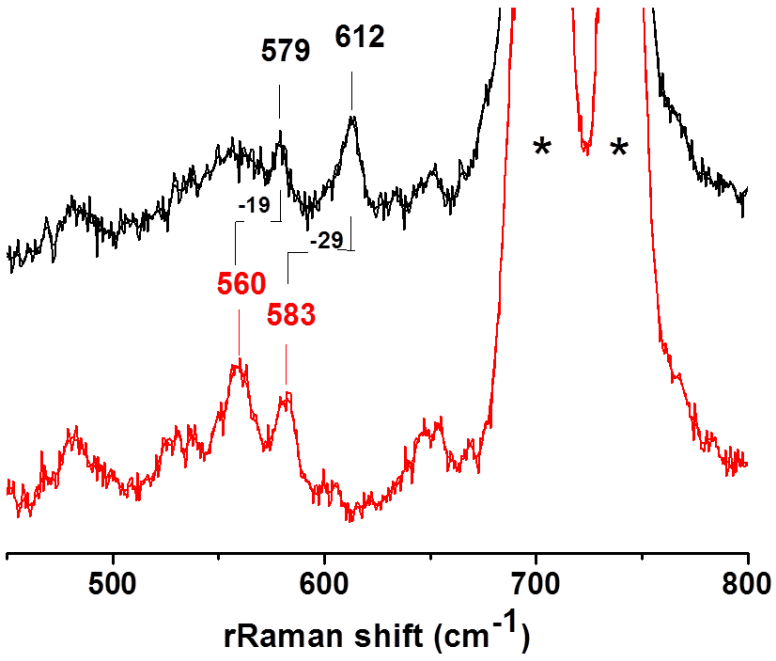

Figure S 4. Raman shifts obtained using a 413 nm laser excitation for **3b** with $^{16}O_2$ (top), and $^{18}O_2$ (bottom). Bands originating from the solvent are marked by asterisks.

II. Kinetic plots of 3a *vs.* substrate concentration

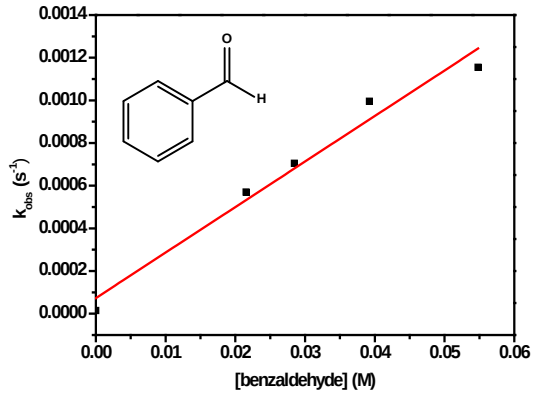

$k_2(-60^{o}C)=0.021\ M^{-1}s^{-1}$

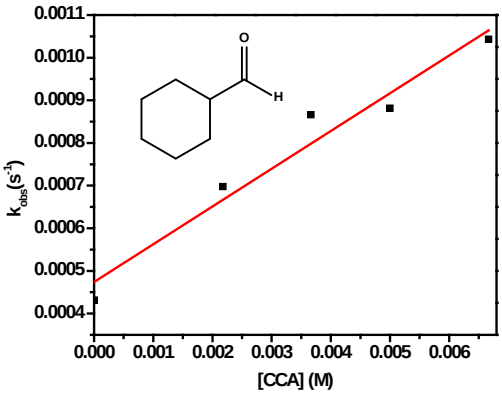

$k_2(-60^{o}C)=0.088M^{-1}s^{-1}$

Figure S 5. Pseudo first-order rate constants as a function of substrate concentration the reaction of **3a** with benzaldehyde (left) and CCA at -60°C in CH_2Cl_2

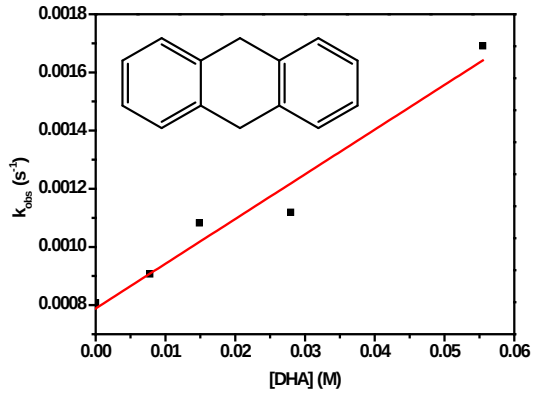

$k_2(-60^{o}C)=0.015\ M^{-1}s^{-1}$

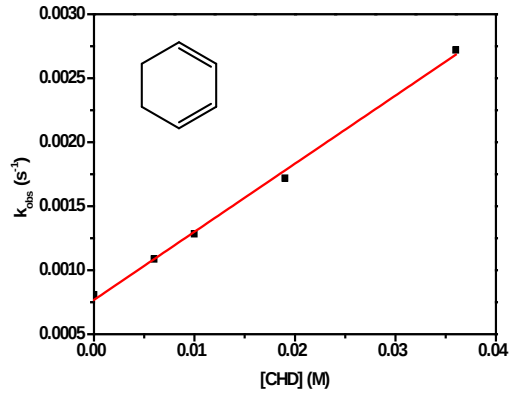

$k_2(-60^{o}C)=0.053\ M^{-1}s^{-1}$

Figure S 6. Pseudo first-order rate constants as a function of substrate concentration the reaction of **3a** with dihydroanthracene (left) and 1,3 cyclohexadiene (right) at -60°C in CH_2Cl_2.

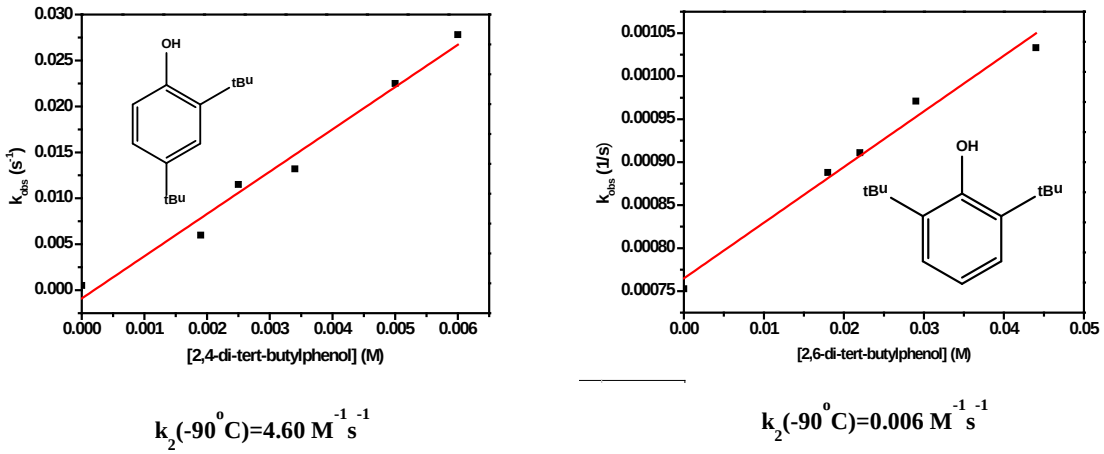

$k_2(-90^{o}C)=4.60\ M^{-1}s^{-1}$ $k_2(-90^{o}C)=0.006\ M^{-1}s^{-1}$

Figure S 7. Pseudo first-order rate constants as a function of substrate concentration the reaction of **3a** with 2,4-di-*tert*-butylphenol (left) and 2,6-di-*tert*-butylphenol (right) at -90°C in CH_2Cl_2.

III. Kinetic plots of 3b *vs.* substrate concentration

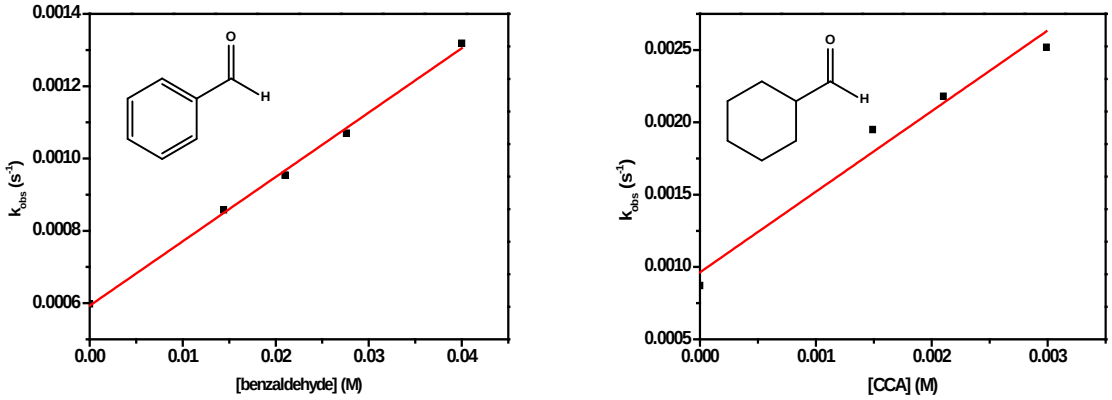

$k_2(-60^{o}C)=0.0178\ M^{-1}s^{-1}$ $k_2(-60^{o}C)=0.557\ M^{-1}s^{-1}$

Figure S 8. Pseudo first-order rate constants as a function of substrate concentration the reaction of **3b** with benzaldehyde (left) and cyclohexane carboxaldehyde (right) at -60°C in CH_2Cl_2.

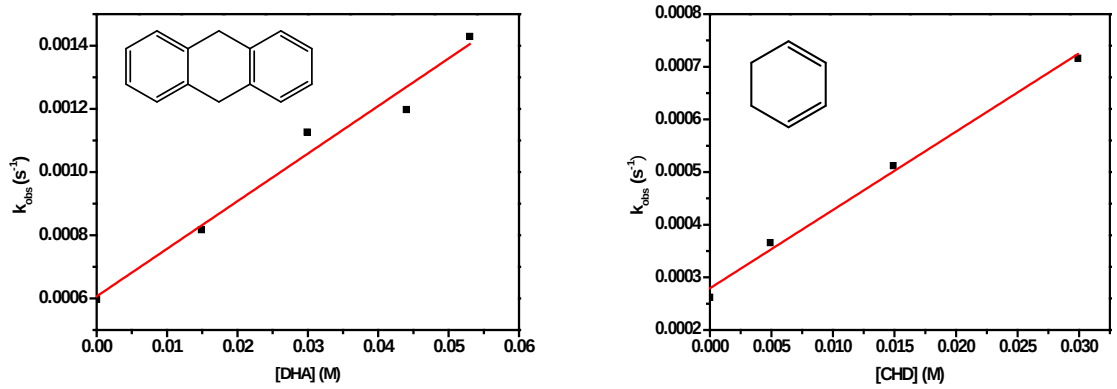

$k_2(-60^{o}C)=0.015\ M^{-1}\ s^{-1}$ $k_2(-60^{o}C)=0.0148\ M^{-1}\ s^{-1}$

Figure S 9. Pseudo first-order rate constants as a function of substrate concentration the reaction of **3b** dihydroanthracene (left) and 1,3 cyclohexadiene (right) at -60°C in CH_2Cl_2.

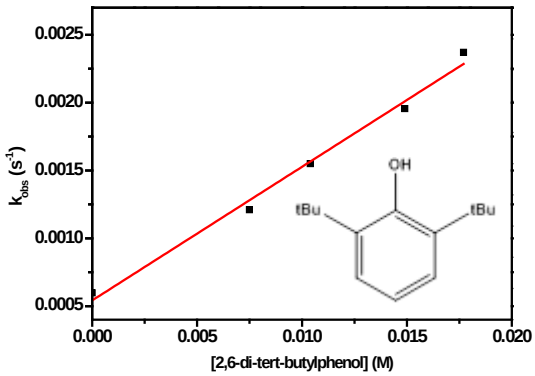

$k_2(-60^{o}C)=0.098\ M^{-1}\ s^{-1}$

Figure S 10. Pseudo first-order rate constants as a function of substrate concentration the reaction of **3b** 2,6-di-*tert*-butylphenol (right) at -60°C in CH_2Cl_2.

IV. Products obtained after reaction of 3b with electrophilic and nucleophilic substrates

Table S1: Reaction of **3b** with various electrophilic and nucleophilic substrates

Substrate	Products
DHA	Anthracene (45%)
CHD	Benzene (49%)
2,4-DTBP	2,2',4,4'-tetra-*tert*-butyl-6,6'-biphenol (82%)
2,6-DTBP	2,2',6,6'-tetra-*tert*-butyl-4,4'-biphenol (85%)
CCA	cyclohexene (62%) + Formate

V. DFT Calculations on 3a and 3b

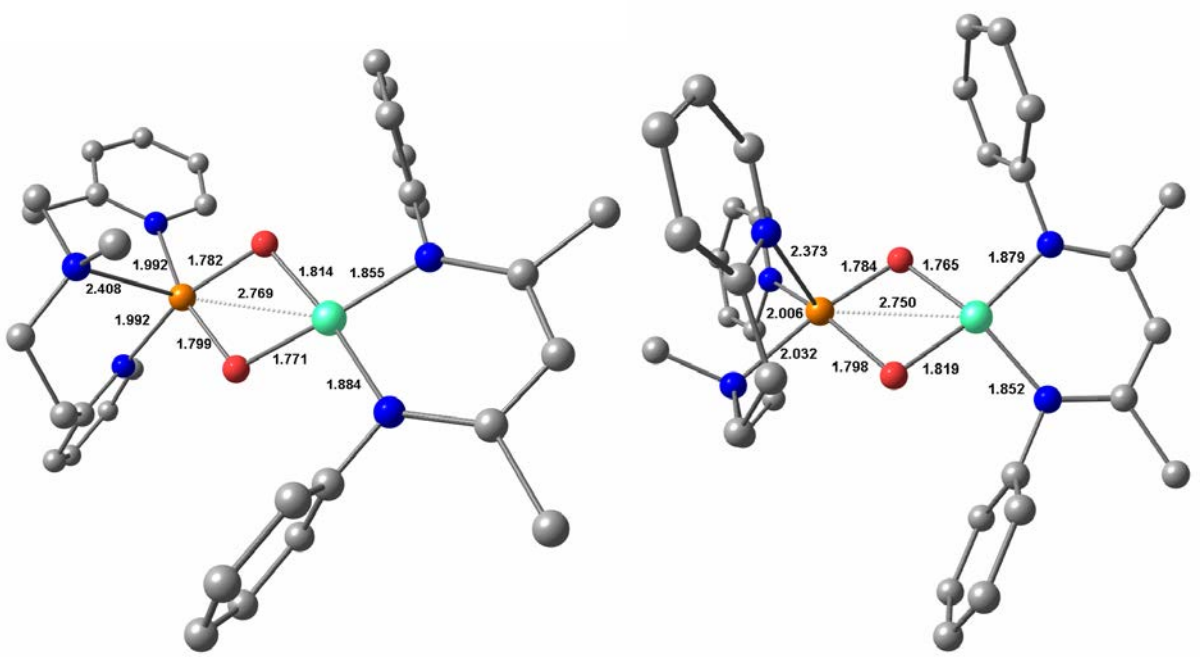

Figure S 11 Optimized molecular structures for **3b**; Conformer A (left) and B (right).

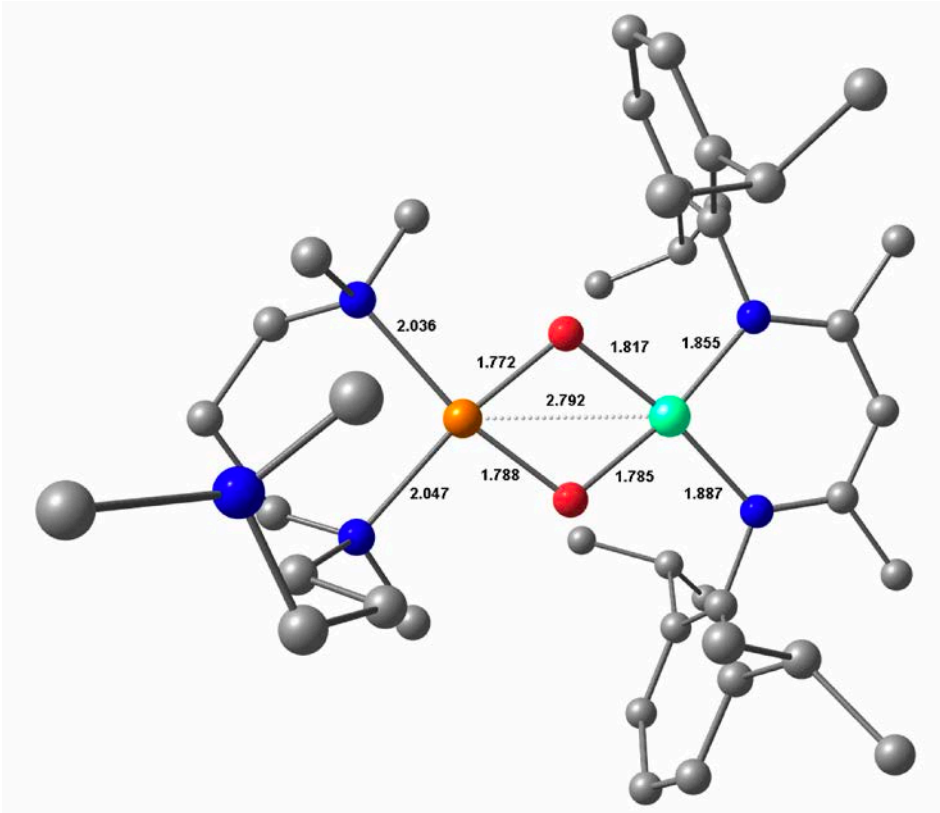

*Figure S 12 Optimized molecular structure for **MEAN.***

Metrical parameters and Gibbs free energies

Table S 2. Calculated metrical parameters for the **3a** and **3b** conformers and the previously reported $[LNi^{III}O_2Cu^{III}(MeAN)]^+$ complex.

Species	**3a**		**3b**		**MEAN**
Parameter	**(A)**	**(B)**	**(A)**	**(B)**	
Cu-Ni	2.758	2.857	2.769	2.750	2.792
Cu-O1	1.781	1.944	1.782	1.784	1.772
Cu-O2	1.802	1.817	1.799	1.798	1.788
Cu-N1	1.980	2.077	1.992	2.006	2.036
Cu-N2	1.966	2.095	1.992	2.032	2.047
Cu-N3	2.514	2.072	2.408	2.373	-
Ni-O1	1.815	1.817	1.814	1.765	1.817
Ni-O2	1.764	1.751	1.771	1.819	1.785
Ni-N4	1.861	1.854	1.855	1.879	1.855
Ni-N5	1.895	1.887	1.884	1.852	1.887
O1-Cu-O2	79.1	74.6	78.8	79.7	77.9
N1-Cu-N2	95.1	136.9	96.5	90.0	98.2
O1-Cu-N1	90.6	111.1	89.5	93.5	90.6
O2-Cu-N2	91.5	92.6	91.7	93.3	93.3
O1-Cu-N3	104.7	99.3	107.5	101.0	-
O2-Cu-N3	106.0	173.7	101.3	107.0	-
O1-Ni-O2	79.2	79.5	78.7	79.6	76.8
N4-Ni-N5	95.4	95.3	95.4	95.4	95.3
O1-Ni-N4	93.0	92.5	93.6	93.8	93.3
O2-Ni-N5	93.4	92.8	94.4	92.7	94.7
O1-N4-N5-O2	11.2	3.7	16.2	14.3	4.5

Table S 3. Calculated Gibbs free energies for the **3a** and **3b** conformers

	Conformer	Energy (Eh)	Stability (kcal/mol)	Favored species
3a	**(A)**	-5121.457043	0	Conformer (A)
	(B)	-5121.372839	**52.8**	
3b	**(A)**	-4813.04405014	0	Conformer (A)
	(B)	-4813.02925132	**9.30**	

Spin densities and SOMOs

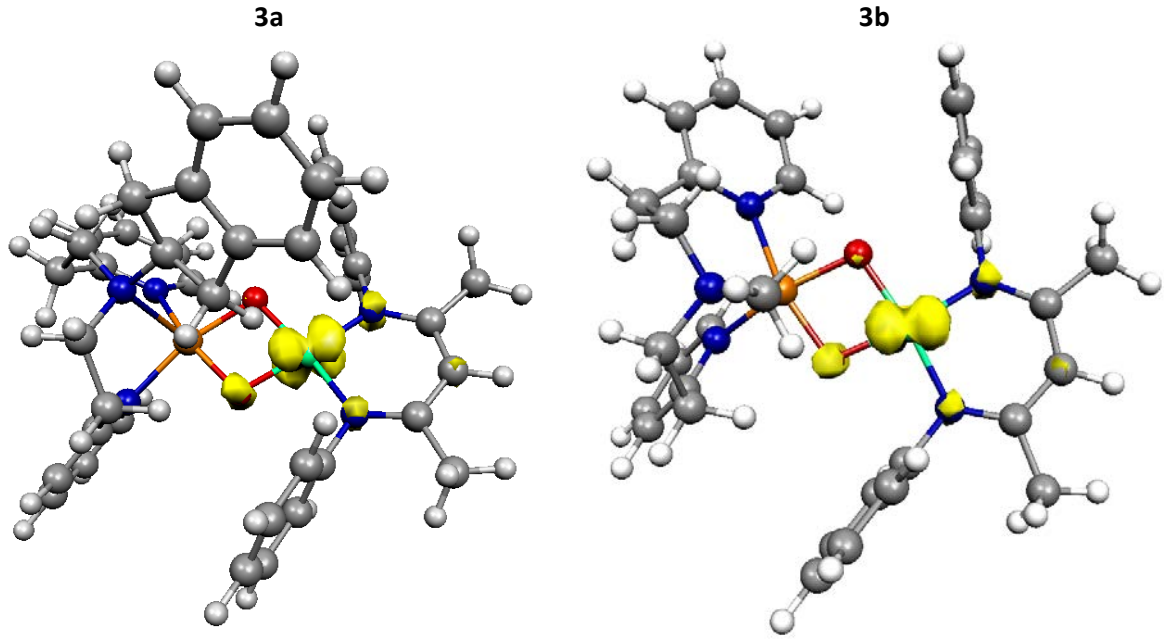

Figure S 13. Spin density plots of **3a** and **3b** conformer (A)

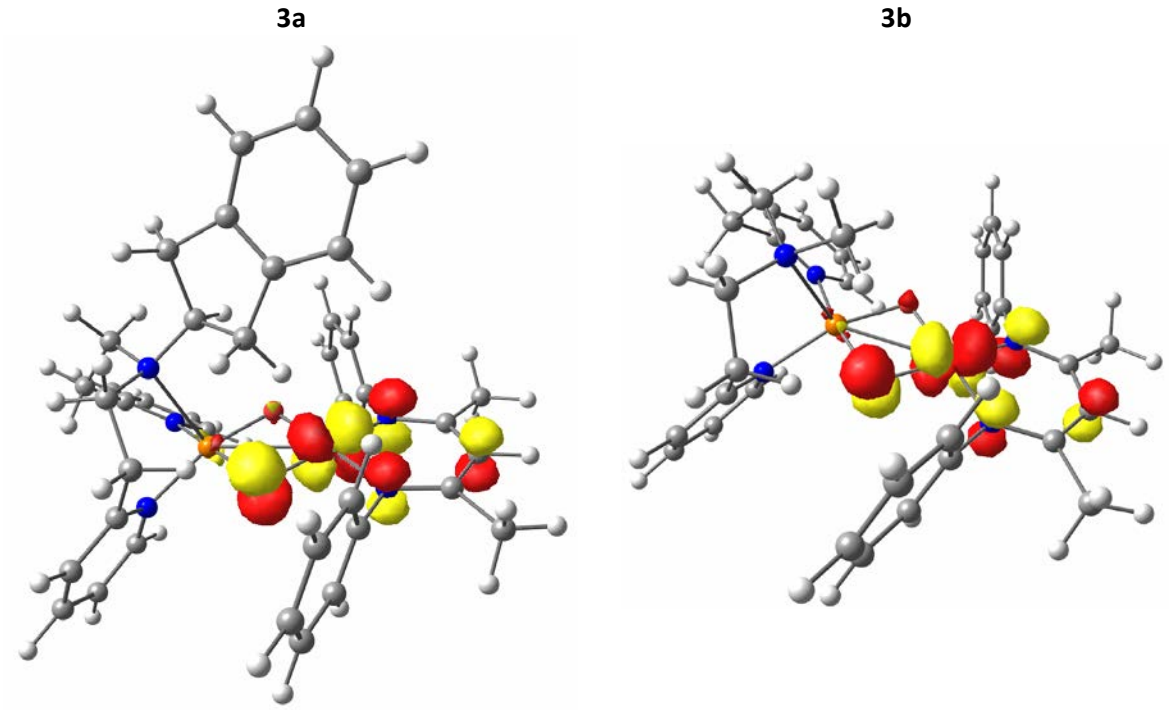

Figure S 13. Singly Occupied Molecular Orbitals of **3a** and **3b** (conformer A)

Spectroscopic parameters

Table S 4. Comparison between calculated and experimental EPR parameters for **3a** and **3b** conformer (A)

g_1; g_2; g_3; (g_{av})	**3a**	**3b**
Expt.	2.006; 2.140; 2.410 (2.185)	2.006; 2.130; 2.390 (2.175)
Calc.	2.067; 2.129; 2.282 (2.160)	2.061; 2.124; 2.280 (2.155)

Table S 5. Comparison between calculated and experimental Raman shifts for **3a** and **3b** conformer (A)

ν ($\Delta[^{18}O_2]$) (cm^{-1})	**3a**		**3b**	
Expt.	605 (-31)	556 (-21)	612 (-29)	579 (-19)
Calc.	596 (-22)	553 (-7)	621 (-21)	528 (-6)

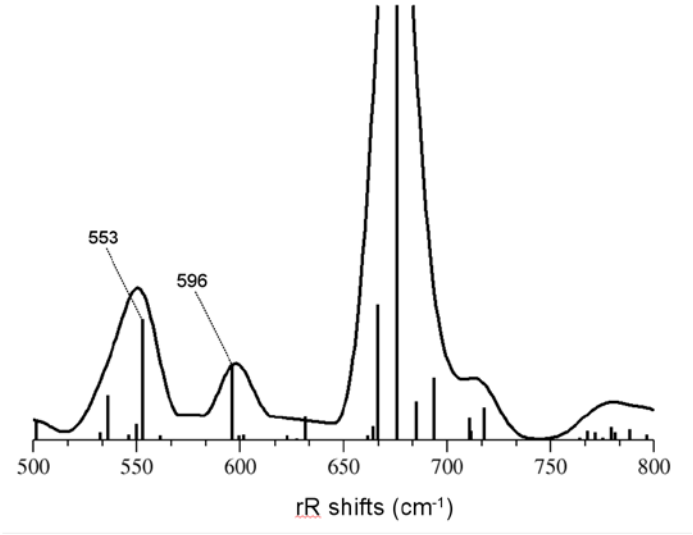

Figure S 14. Computed Raman spectrum for **3a** in the presence of 16-O_2.

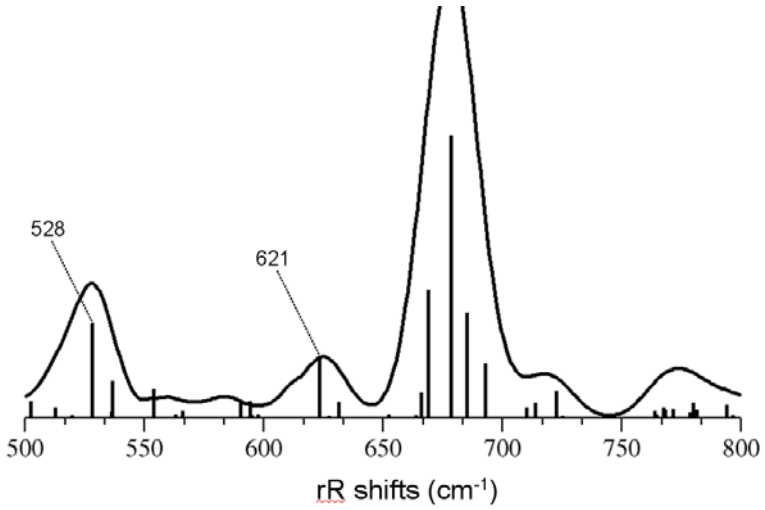

Figure S 15. Computed Raman spectrum for **3b** in the presence of 16-O_2.

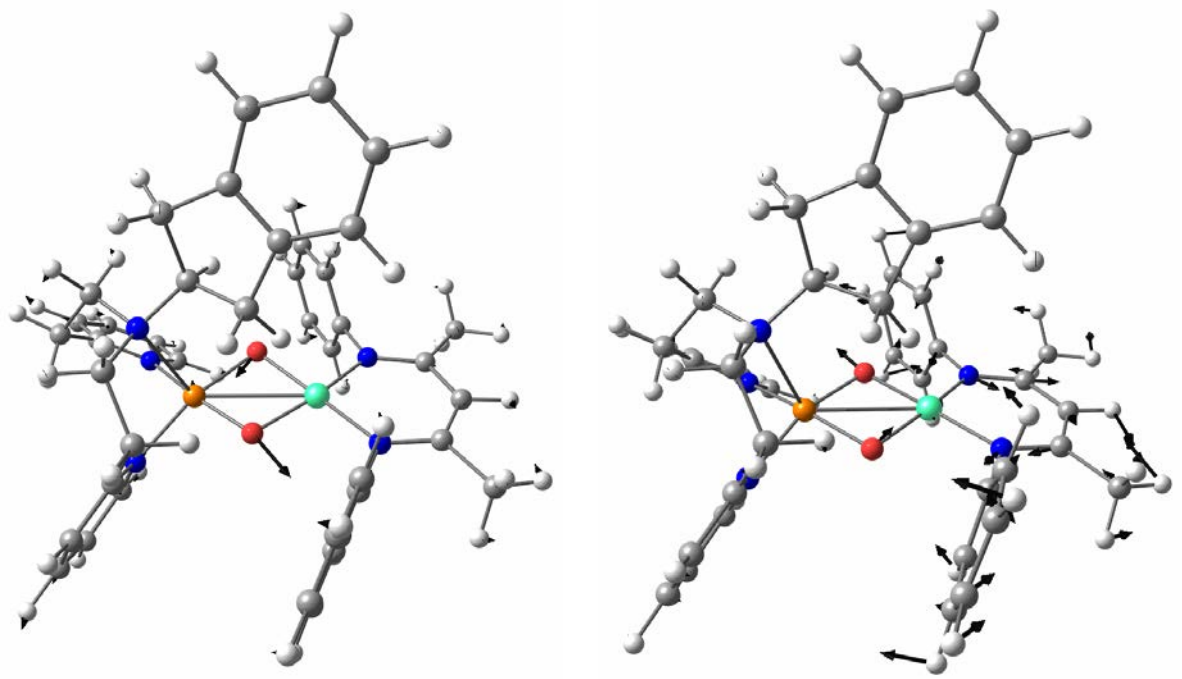

Figure S 16. Normal modes relevant to the 596 cm^{-1} (left) and 553 cm^{-1} (right) Raman shifts of **3a**

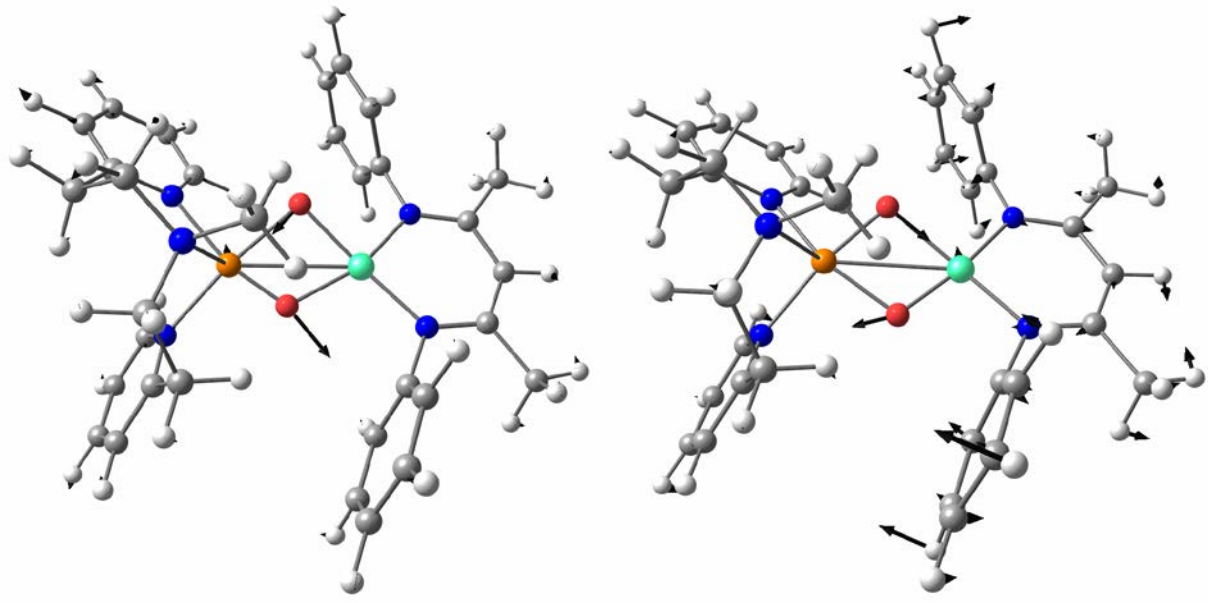

Figure S 17. Normal modes relevant to the 621 cm^{-1} (left) and 528 cm^{-1} (right) Raman shifts of **3b**

Total density and individual Natural Charges

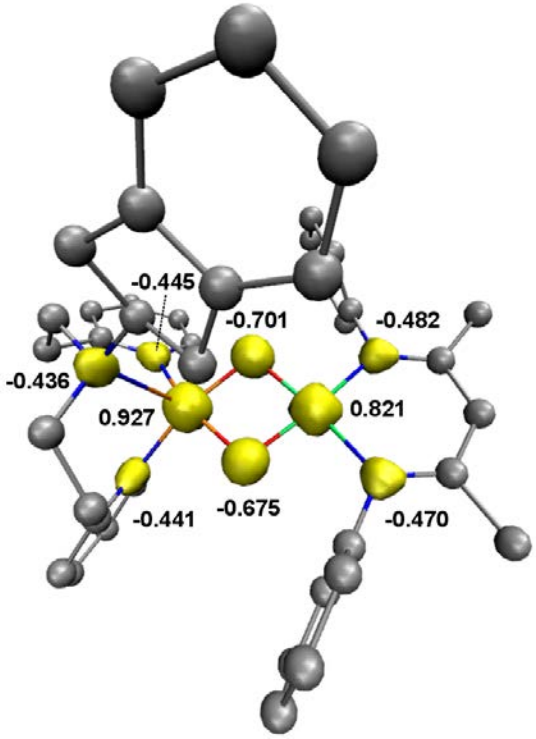

Figure S 18. Total density and individual natural charges for **3a**.

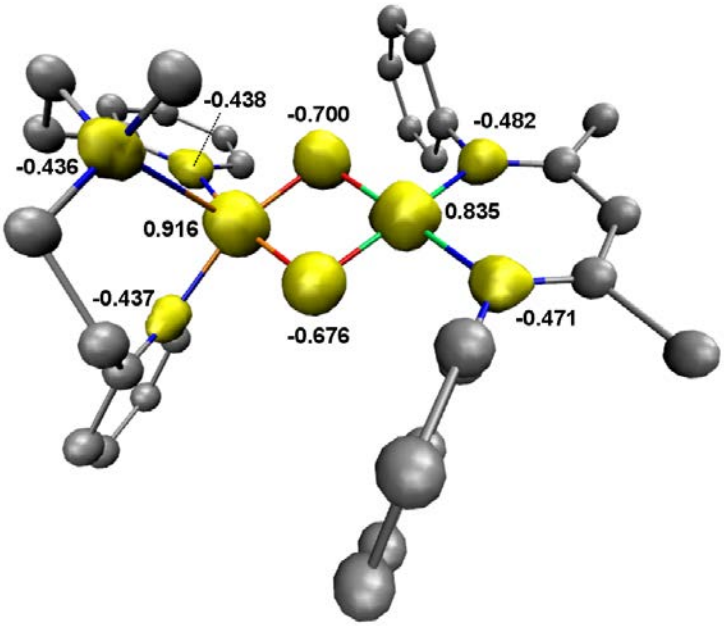

Figure S 19. Total density and individual natural charges for **3b**.

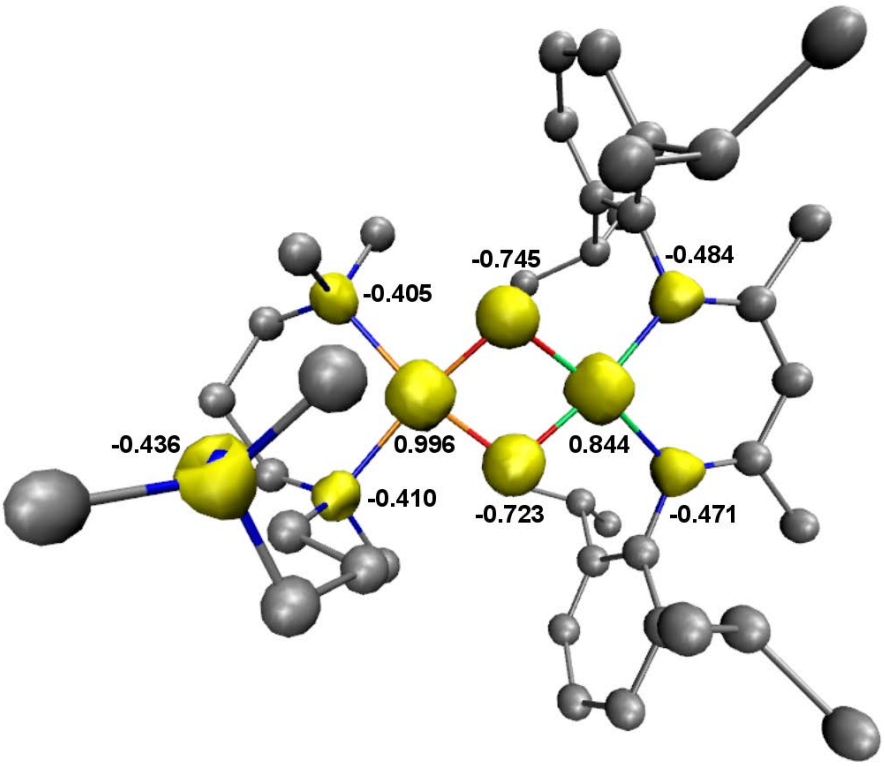

Figure S 20. Total density and individual natural charges for $[LNi^{III}O_2Cu^{III}(MeAN)]^+$.